

LA-UR-01-5818

Approved for public release;
distribution is unlimited.

Title:

INVESTIGATION OF THE MORLET WAVELET FOR NONLINEARITY DETECTION

Author(s):

Amy N. Robertson

Submitted to:

<http://lib-www.lanl.gov/la-pubs/00796554.pdf>

Los Alamos National Laboratory, an affirmative action/equal opportunity employer, is operated by the University of California for the U.S. Department of Energy under contract W-7405-ENG-36. By acceptance of this article, the publisher recognizes that the U.S. Government retains a nonexclusive, royalty-free license to publish or reproduce the published form of this contribution, or to allow others to do so, for U.S. Government purposes. Los Alamos National Laboratory requests that the publisher identify this article as work performed under the auspices of the U.S. Department of Energy. Los Alamos National Laboratory strongly supports academic freedom and a researcher's right to publish; as an institution, however, the Laboratory does not endorse the viewpoint of a publication or guarantee its technical correctness.

INVESTIGATION OF THE MORLET WAVELET FOR NONLINEARITY DETECTION

Amy N. Robertson

Engineering Analysis Group (ESA-EA)
MS P946
Los Alamos National Laboratory
Los Alamos, NM 87545

ABSTRACT

Frequency response functions (FRFs), typically calculated by means of the Fourier transform, are used extensively throughout structural dynamics to identify modal characteristics of a structure. Fourier methods work well with linear systems, but have limitations when nonlinearities are present, largely due to their inability to examine non-stationary data. A nonlinear system is often characterized by the variation of its structural response in time. More recently, wavelets have been introduced as an alternative method to FRF calculation. Unlike Fourier methods, wavelets are a time/frequency transform, allowing for the creation of a time-varying FRF. This paper explores the use of wavelet-based FRFs to identify nonlinear behavior in an eight degree-of-freedom spring-mass structure. Examination of temporal changes in the higher frequency range are used to determine the location of the system's nonlinearities.

NOMENCLATURE

$\Psi(t)$	Mother wavelet
a	Scaling parameter
b	Translation parameter
$W_x(a,b)$	Wavelet transform
FRF	Frequency response function
$H(w)$	Fourier-based FRF
$H_w(f,t)$	Wavelet-based FRF
ST	Standard Deviation in time of wavelet FRF summed over all frequencies

INTRODUCTION

Every real system will exhibit some degree of non-linear behavior. Nonlinearities are common in flexible structures, systems with friction, or ones with compliant materials and may be categorized as geometric, kinematic, or material-based. In many circumstances, an increase in the nonlinearity of a system can indicate a change that might affect the health or operation of the system. Finding

methods that are able to identify and locate these changes are of great importance.

Fourier-based methods have been used extensively throughout structural dynamics for the extraction of modal properties. Specifically, frequency response functions are often used as a means for identification and comparison of the averaged modal characteristics of a structure. For linear systems, this has been a successful measurement device, but does not typically perform well when nonlinearities are present. A nonlinear system can be identified by the variation of its structural response in time. With Fourier-based methods, the frequency content of the signal is typically averaged over a large number of data blocks, smearing out characteristics, and eradicating all time information. Time/frequency transformations alleviate this problem by providing information on how the frequency content of a signal changes in time. Of these transformations, wavelets have been gaining popularity in recent years due to the attractive inverse relationship of frequency and time. At lower frequencies, a fine frequency resolution is provided with a coarser time resolution. This relationship is inverted at higher frequencies, where time resolution is increased and frequency decreased. Examination of changes in the higher frequencies of an FRF is a good indication of the occurrence of certain types of nonlinearities present in a system. Wavelets naturally scale themselves appropriately for this type of analysis.

This paper seeks to identify damage induced into an 8-dof spring-mass test system. This system, explained in detail in [1], consists of eight masses sliding on a steel rod, interconnected by linear springs. Damage is simulated in the system by the addition of small bumpers that limit the compression of the springs. Morlet wavelets are investigated as a means for identifying the damage in the system. The Morlet wavelet is a complex valued transform that captures both the magnitude and phase characteristics of a signal while also retaining its temporal nature. This transform can be used to form frequency response functions whose temporal nature can be used to identify damage.

This paper builds upon the work performed by Hartin [1] on applying wavelet-based FRFs to the analysis of a bilinear structure. In this paper, Hartin shows how wavelet FRFs can be used to identify the location of a nonlinearity in a simulated system using bifurcated modes. His work shows

much promise for the use of wavelet-based FRFs in the identification of nonlinearities or damage present in a system.

Other approaches have been used to analyze this eight degree-of-freedom structure or ones similar, including papers by Sohn [2], Bement and Farrar [3], Wait, et al [4], and Hunter [5]. The methods used in these papers include time-based analysis of the system response and statistical methods for evaluating the modal properties. The results of this work have been promising, but wavelets offer a new avenue of examination into the time variability of the spectral nature of the system, which these approaches cannot take advantage of.

METHOD

In the example that will be examined in this paper, a nonlinearity is induced into a system through contact bumpers. This impact-type nonlinearity adds high frequency content to the response spectrum of the system. Traditional Fourier methods used to determine the frequency response identify the lower frequency components quite well, which is where the fundamental modes of the system are located. The high frequency content, however, is usually much lower in magnitude and therefore harder to identify. The system itself works as a weak low-pass filter, primarily transmitting the lower frequency content.

Even if a definite change in the frequency spectrum can be identified with and without the nonlinearity present, further difficulty comes in trying to identify its exact location. Since the system analyzed in this paper is essentially discrete (all degrees of freedom are measured), traditional methods that analyze the frequency spectrum have great potential to locate the damage. For more realistic systems with limited measurement degrees of freedom, however, this becomes more difficult.

By looking at the standard deviation in time of the high frequency content, the exact location of the damage can be seen. Wavelets are able to show how the FRF changes in time and this will be used to identify the location of the nonlinearity or damage in the system.

This identification procedure is specific to impact type nonlinearities or any other feature that would excite high frequency vibrations in a system. But, usually the best features for damage identification, or in this case nonlinearity detection, are those that are application specific.

WAVELET BASED FRFS

Wavelets are mathematical functions that decompose a signal into scaled coefficients using a set of wavelet basis functions. This is very similar to Fourier transforms which use dilations of sinusoids as the bases. The family of basis functions used for wavelet analysis is created by both dilations (scaling) and translations (in time) of a "mother wavelet", thereby providing both time and frequency information about the signal being analyzed. There are many different functions that can be called wavelets. In this report, the Morlet wavelet is used:

$$\Psi(t) = e^{(-\sigma^2 t^2 - i2\pi f_0 t)} \quad (2)$$

which is very similar to a sinusoid with a Gaussian envelope. The term f_0 is the center frequency of the sinusoid and σ determines the width of the frequency band. The wavelet transform is obtained by convolving the signal $x(t)$ with the translations (b) and dilations (a) of the mother wavelet:

$$W_x(a, b) = \int_{-\infty}^{+\infty} x(t) \Psi_{a,b}^* dt \quad (3)$$

Since the Morlet wavelet is able to compute both magnitude and phase characteristics of a signal while also retaining its temporal nature, it can be used to form wavelet-based frequency response functions (or transmissibility functions) that retain the variability of the system in time. The complex form of the Morlet wavelet is unique compared to other wavelets, and allows for the computation of modal properties.

The frequency response function relates the output response of a system to its input and is usually calculated using the Fourier transform:

$$H(w) = \frac{Y(w)}{X(w)} \quad (4)$$

The Fourier Transform has the unique characteristic of transforming a convolution into a multiplication, which allows for the simple formula shown above. Time domain methods, and non-complex wavelet-based methods do not have this quality and are therefore computationally expensive. This is compounded further when dealing with noisy data. The most common method for calculating an FRF for noisy data is the H1 formulation which assumes that noise is present on the output signal only:

$$H(w) = \frac{Y(w)X^*(w)}{X(w)X^*(w)} \quad (5)$$

The H1 FRF may also be formed using a complex wavelet transform. Transforms of the input and response signals are calculated with Equation 3 and then used to form the spectral densities ($Y(w)X^*(w)$ and $X(w)X^*(w)$) shown in Equation 5:

$$H_w(f, t) = \frac{W_y(a, b)W_x^*(a, b)}{W_x(a, b)W_x^*(a, b)} \quad (6)$$

This formulation was implemented numerically using the method detailed by Wang and McFadden [6] who utilize Fourier transforms to perform the integration in Equation 3.

The time resolution of the wavelet-based FRF is traded-off with its frequency resolution. The center frequency f_0 and bandwidth, which determines the scale parameter of the

wavelet transform, can be varied to develop an optimal time-frequency resolution.

At one extreme, one can obtain an FRF with absolutely no time resolution, which will look almost identical to the FRF formed by the more traditional Fourier transform. This can be achieved by averaging the wavelet-based FRF in the time domain, which allows for a smoother function in the frequency domain. Averaging is performed on the phase and magnitude of the FRF. Equation 7 shows how time averaging of the magnitude of the FRF is performed with an ensemble length of size m :

$$\bar{H}_w(f, t_k) = \sum_{i=m^*(k-1)+1}^{m^*k} |H_w(f, t_i)| \quad (7)$$

EXPERIMENTAL ANALYSIS

An eight degree-of-freedom system (Figures 1 and 2) was constructed to study the effectiveness of various vibration-based damage identification techniques [1]. The system consists of eight masses sliding on a steel rod interconnected by linear springs. Non-linear damage is simulated by placing rods (bumpers) on one mass, which limits the amount of relative motion between it and the adjacent mass. A small clearance is maintained between the rods and adjacent masses and impact occurs when the mass translates further than the clearance. This impact simulates spring deterioration which would permit contact between adjacent masses to occur. It could also approximate the impact from the opening and closing of a crack during vibration or the rattling of a loose joint. The degree of damage can be altered by changing the size of the bumpers, hence allowing for a larger or smaller clearance between adjacent masses.

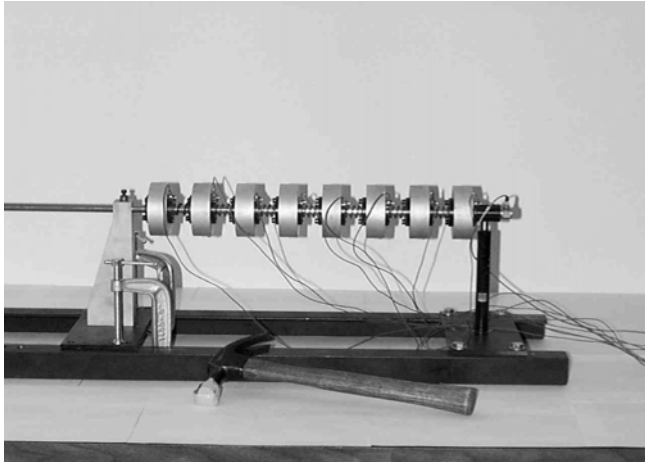


Figure 1: Picture of Eight Degree-of-Freedom System

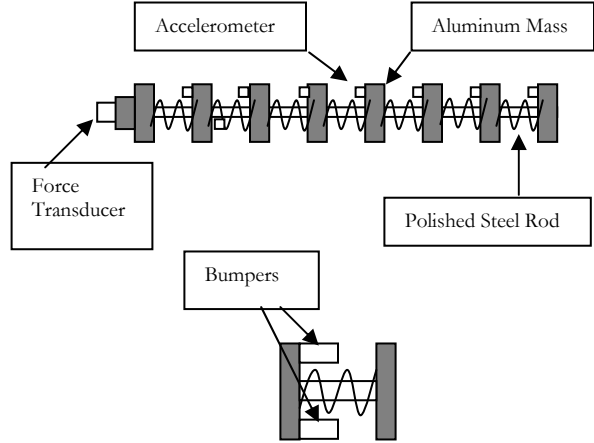


Figure 2: Schematic of Eight Degree-of-Freedom System and Simulated Damage

The system was excited at the first degree of freedom using a Gaussian random signal supplied by a shaker along the axis of the steel rod. Acceleration responses were measured at each of the eight degrees of freedom using accelerometers. A series of experiments were run with varying excitation magnitudes, clearance levels, and bumper locations. Bumpers were placed at three different positions: between masses 1 and 2, masses 5 and 6, and masses 7 and 8. For each of these locations, eight experiments were analyzed as summarized in Table 1. A range of excitation voltages were actually used, but only the 6 and 7 volt levels will be analyzed due to their good measurement quality as compared to the other levels.

Case	Bumper Clearance	Excitation Voltage
1	No Bumper	7V
2	No Bumper	6V
3	0 mm	7V
4	0.2 mm	7V
5	0.4 mm	7V
6	0 mm	6V
7	0.2 mm	6V
8	0.4 mm	6V

Table 1: List of Experimental Cases Performed

FRF Estimation

Frequency response function estimates for the system without any bumpers present are given in Figure 3 for the acceleration at mass 1 due to the input force. The Fourier

based estimate was calculated by averaging 8 ensembles

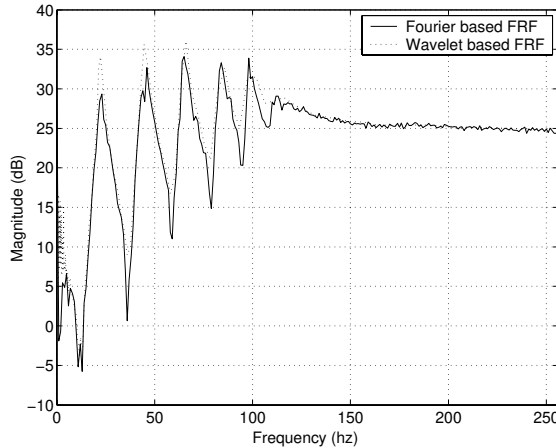


Figure 3: Frequency Response Function Magnitude for Input 1/Output 1 Without Bumpers (No Damage)

of 512 points each. For comparison, the wavelet method was used to form a purely frequency-domain estimate of the FRF by averaging-out all the time information. This is done using Equation 7 with an ensemble length of 4096, or the entire time-span of the function.

Unlike the work done by Hartin [1], this data is not simulated and therefore contains noise, which necessitates the time-averaging of the wavelet-based FRF to obtain a smooth function. Once averaging is done, the wavelet and Fourier-based FRFs are very similar.

The time-frequency representation of the wavelet-based FRF using only 8 ensemble-averages in time over 0.64 seconds is shown in Figure 4a. The five most prominent modes of the system are clearly visible when compared to the traditional frequency domain plot of the FRF discussed in the last paragraph (shown in Figure 4b). The lack of any high frequency content above the structural modes is characteristic of a linear spring-mass system. The same FRF is examined in Figure 4c with a bumper added between degrees of freedom 1 and 2. The presence of this nonlinearity obviously induces high frequency response in the structure as well as increasing the variability of the response in time. The characteristics shown in this plot are common for all of the damaged cases.

Damage Assessment

The impact of the bumper with the adjacent mass will cause a spike in the time response of the system, thus exciting a wide range of frequencies. This type of damage also causes the system to exhibit nonlinear characteristics, one of which is the excitation of frequencies other than the fundamental modes of the system. Therefore, to assess and locate the nonlinearity or damage in the system, the upper half of the frequency band of the FRF will be examined (128-256 hz). With the ability of the wavelet transform to also provide time

resolution to the FRF, the variability of this function in time will be used as an additional element for the identification of damage in the system.

To quantify the amount of time variability there is in the higher frequencies, the standard deviation (in time) of the FRF at each frequency in the higher frequency band is calculated:

$$std(f_j) = \sqrt{\frac{\sum_{i=1}^n (H_w(f_j, t_i) - \bar{H}_w(f_j, t))^2}{n-1}} \quad (8)$$

These values are then summed to obtain the total standard deviation across all of the higher frequencies, which will be referred to as ST :

$$ST = \sum_{j=n/2+1}^n std(f_j) \quad (9)$$

These calculations were performed for each of the 24 cases mentioned above, which include 3 different locations for the damage: between masses 1 and 2, masses 5 and 6, and masses 7 and 8.

Figure 5a shows the magnitude of the time variability (ST) of the FRF at each output location for the 8 cases when bumpers are placed between masses 1 and 2. A high ST value follows sensor locations 1 and 2 for all cases. This points towards the presence of a nonlinearity between masses 1 and 2. Similar results are given for bumpers placed between masses 5 and 6 (Figure 5b) and masses 7 and 8 (Figure 5c). Especially interesting is the ridge of high frequency response at locations 7 and 8 in Figure 5c.

Figure 6 slices Figure 5c along sensor location 7 to show the relative response for each of the eight cases. Located on the plot are a summary of each case: 7V 0d represents a 7 volt excitation and no damage, while 7V 2gap represents a 7 volt excitation with a bumper clearance of 0.2 mm. From this plot, one can see that the standard deviation in the high frequencies is low when bumpers are not present (cases 1 and 2). Case 3 is the most nonlinear, which has both the largest excitation and the smallest clearance between the bumpers and the adjacent masses.

The results in Figure 5 show clearly that a nonlinearity is occurring and at which sensor location. The ability for the Fourier-based FRF functions to reveal the same information was also assessed. Figure 7 shows the standard deviation (in frequency) of the upper half of the FRF frequency band when bumpers are placed between masses 7 and 8. This value reveals the magnitude of high frequency content for each of the cases. A ridge of high standard deviation values follow sensor location 7, but the relative magnitude between it and the other locations is not as large as the wavelet calculations (Figure 5c). Also in Figure 7 is a ridge of high standard deviation following location 1. This indicates that there is either a high frequency input at location 1 or that

some nonlinearity at that location has produced some locally high frequencies. This result is common to all of the FRF evaluations performed using FFT-based FRFs. It is not understood why this ridge is appearing, but it hampers the ability to locate the damage effectively.

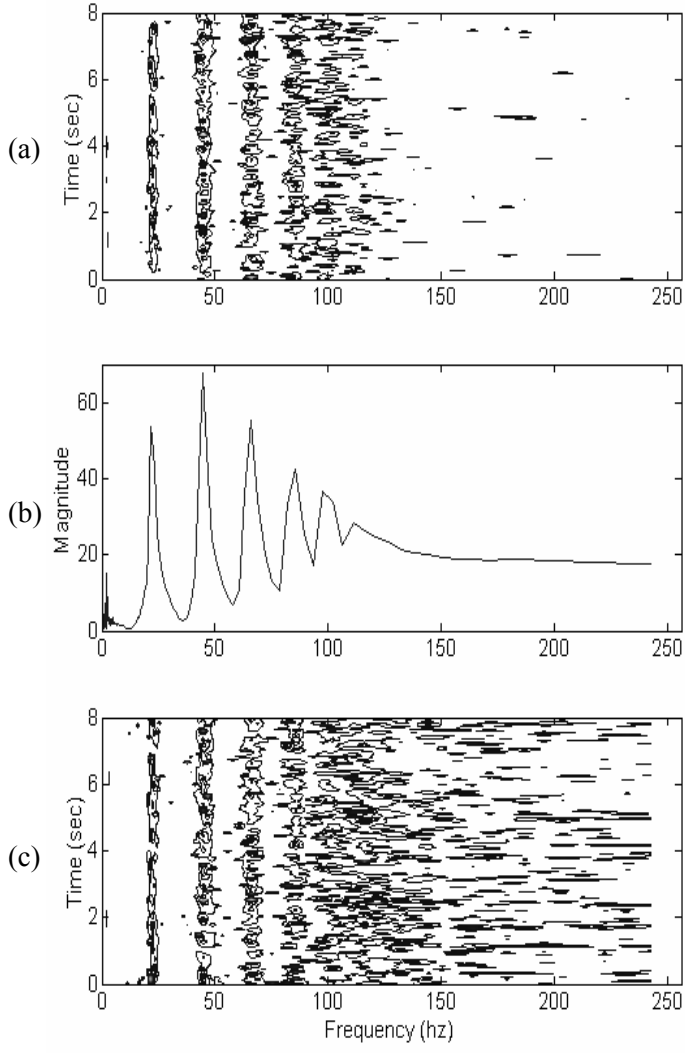


Figure 4: Contour plot of wavelet-based FRF for input 1/output 1 without bumper (a), Wavelet-Based FRF with time resolution averaged out (b), and Wavelet-based FRF for input 1/output 1 with bumper between DOFs 1 and 2 (c)

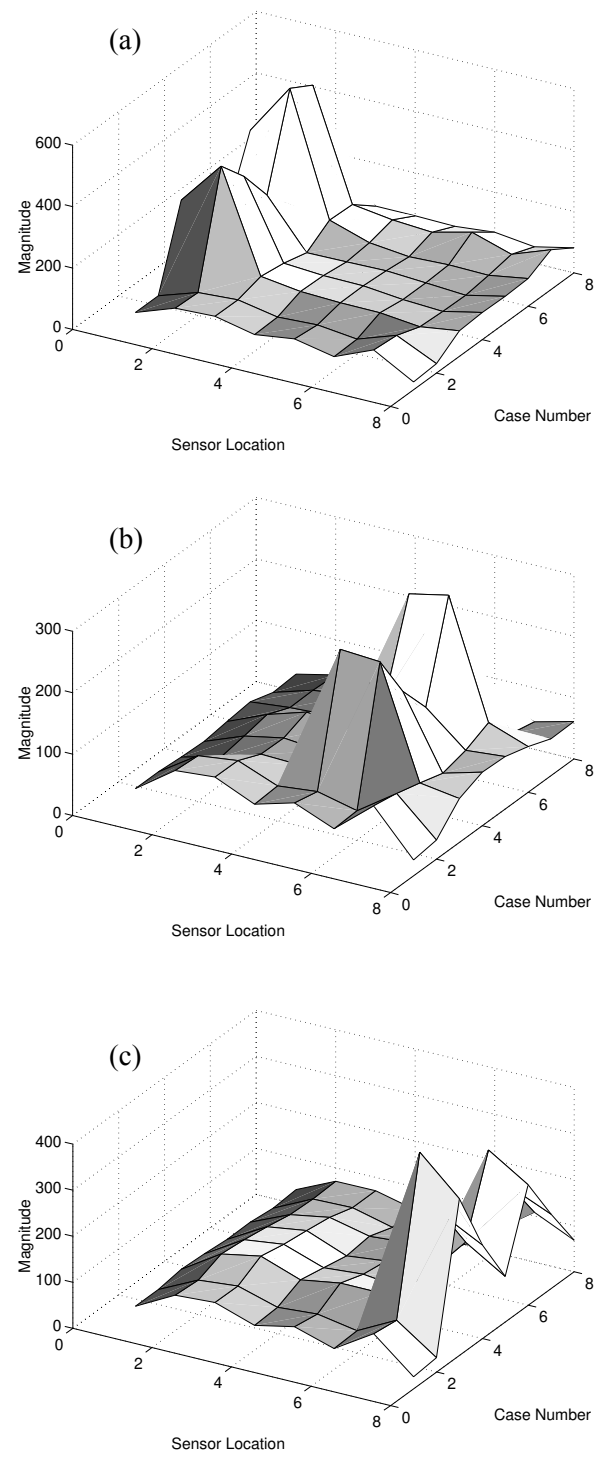


Figure 5: ST-value at each sensor location and case number for : Bumpers between masses 1 and 2 (a), Bumpers between masses 5 and 6 (b), and Bumpers between masses 7 and 8 (c)

ACKNOWLEDGEMENTS

I would like to thank Dr. John Hartin for his help and the use of his Matlab-based software for determining the wavelet-based FRFs.

REFERENCES

1. Hartin, John R., "Application of a Wavelet Based FRF to the Analysis of a Bilinear Structure", Proceedings of the 19th International Modal Analysis Conference, Vol 2, 1414-1419, 2000.
2. Sohn H., Farrar, C.R., "Time Series Analyses for Locating Damage Sources in Vibration Systems," Journal of Smart Materials and Structures, Vol. 10, 446-451, Sept. 2001.
3. Bement, Matthew T. and Farrar, Charles R., "Issues for the Application of Statistical Models in Damage Detection", Proceeding of the 19th International Modal Analysis Conference, Vol 2, 1392-1398, 2000.
4. Wait, J. R.; Arcand, B. Y.; Webster, J. E.; Hunter, N. F., "Identification of Nonlinearities in an 8-DOF System Through Spectral Feedback", Proceedings of the 19th International Modal Analysis Conference, Vol 2, 970-976, 2000.
5. Hunter, N. F., "Bilinear System Characteristics from Nonlinear Time Series Analysis", Proceedings of the 17th International Modal Analysis Conference, 1488-1494, 1997.
6. W.J. Wang and P.D. McFadden, "Application of Wavelets to Gearbox Vibration Signals for Fault Detection", Journal of Sound and Vibration, 192 (5), 927-939, 1996.

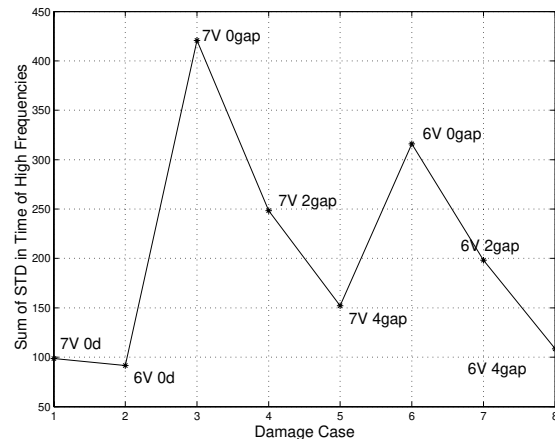


Figure 6: ST Values at Sensor Location 7 for Wavelet-Based FRF with Bumpers Between Masses 7 and 8.

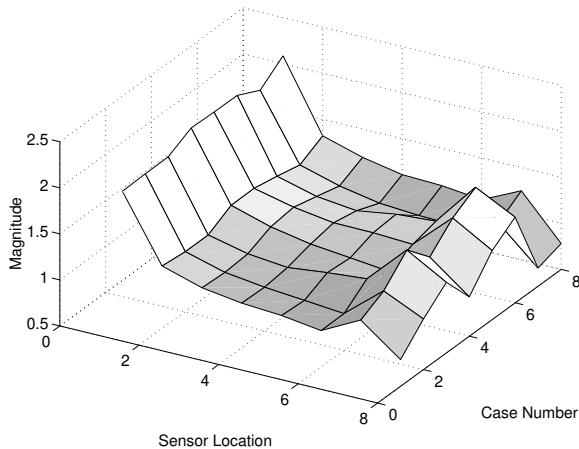


Figure 7: Standard deviation of the upper frequency range of the Fourier-Based FRF with bumpers between masses 7 and 8.

CONCLUSIONS

This paper has shown the possibility of using wavelet-based frequency response functions for damage or nonlinearity assessment. The time information obtained by using wavelets instead of traditional Fourier transforms to form the FRFs allows for a clear indication of where damage is occurring in the system. This example illustrates the ability to distinguish damage induced by impact-type nonlinearities. This type of damage is of great concern in many applications, but this procedure might not readily apply in other areas of nonlinearity detection. The ability to apply this procedure to real test data that includes noise is encouraging. Further applications of this procedure to more complicated test structures would provide for a more insightful evaluation.